19th International Conference on the Computation of Electromagnetic Fields

Technical Program

Compumag 2013

30 June–4 July 2013, Budapest, Hungary

PA4-12
A Multi-objective Repository-based Genetic Algorithm for Ultra-wideband Antenna Optimization
Cláudio Silva, Sinara Martins
Federal University of Rio Grande do Norte (UFRN), Brazil

PA4-13
Statistical Moment-based Robust Design Optimization for Nonlinear Electromagnetic Devices
Su-gil Cho, Junyong Jang, Tae Hee Lee
Hanynag University, Republic of Korea (South Korea)

PA4-14
Meaning of the Rational Solution Obtained by Game Theory
Tomoyuki Miyamoto[1], Shinya Matsutomo[2], Fumiaki Nobuyama[1], So Noguchi[1]
[1]Hokkaido University, Japan; [2]Niihama National College of Technology, Japan

PA4-15
Optimal Rotor Structure of Surface-mounted Permanent Magnet Motor for Vibration Reduction
Sunghoon Lim, Seungjae Min, Jung-Pyo Hong
Hanyang University, Republic of Korea (South Korea)

PA4-16
A Parallel Version of the Self-Adaptive Low-High Evaluation Evolutionary-Algorithm for Electromagnetic Device Optimization
Emanuele Dilettoso, Santi Agatino Rizzo, Nunzio Salerno
DIEEI - Università di Catania, Italy

PA4-17
Embedded Multilevel Optimization for Nonlinear Time Stepping Mesh based Reluctance Network
Maya Hage Hassan, Guillaume Krebs, Ghislain Remy, Claude Marchand
Laboratoire de génie électrique de Paris, France

PA4-18
Low Cogging Torque Design of Permanent-Magnet Machine using Modified Multi-level Set Method with Total Variation Regularization
Piotr Putek[1], Piotr Paplicki[2], Ryszard Palka[2]
[1]Ghent University, Belgium; [2]West Pomeranian University of Technology, Poland

PA4-19
A Numerically Efficient Reliability-Based Robust Optimal Design Algorithm: Application to TEAM 22
Ziyan Ren, Chanhyuk Park, C.S. Koh
Chungbuk National University, Republic of Korea (South Korea)

Optimal Rotor Design of Surface-mounted Permanent Magnet Motor for Vibration Reduction

Sunghoon Lim, Seungjae Min and Jung-Pyo Hong

Department of Automotive Engineering, Hanyang University, Seoul, 133-791, Korea

This paper presents a new optimization method to design a rotor structure for a surface-mounted permanent magnet (SPM) motor that can reduce vibration. The optimization problem is formulated with a multi-objective function to minimize the fluctuation of the radial magnetic force and the torque ripple. To obtain the optimal rotor shape consisting of a permanent magnet and ferromagnetic material, a multiple level set model is employed to express the structural boundaries and magnetic properties of each material. The updating process of the level set function based on the adjoint sensitivity and the time evolutional equation makes it possible to obtain a novel rotor configuration of the SPM motor. To verify the usefulness of the proposed method, a rotor design example of the SPM motor for electric power steering (EPS) system is performed.

***Index Terms*— Surface-mounted permanent magnet motor, vibration reduction, rotor design, magnetic force, torque ripple, level set method**

I. Introduction

SINCE mechanical vibration is harmful to the robustness of an integration system and generates audible noise, which is a critical factor in human sensitivity, vibration reduction has become an important issue in motor design [1]-[3]. Many studies have noted that the main sources of motor vibration are fluctuation of the magnetic force and mechanical deformation of the motor structure [4]-[5]. Hence, several design techniques such as modification of the motor shape [6]-[7] and pole-slot combination [8] have been proposed to minimize them. Particularly in the surface-mounted permanent magnet (SPM) motor where the permanent magnet (PM) dominates the magnetic flux path, the shape change of the rotor is the key to vibration reduction [9]. Unfortunately, since the magnetic forces that cause the motor's vibration are essential to satisfy the output power, it is very difficult to design a low-vibration rotor shape by using previous approaches because they depend on experimental data and engineering intuition.

In this paper, an optimization method that incorporates localized geometrical change [10] is introduced to get an innovative rotor design that guarantees a decrease in the motor vibration. The level set functions are employed to express the clear boundaries of the rotor and to calculate the magnetic properties of the PM and the ferromagnetic material (FM) [11]. The optimization problem is formulated to minimize the fluctuation of the magnetic forces, such as the local force on the stator and the driving torque, which can cause mechanical deformation of the stator. The volume fraction constraints for each level set function are added to the problem formulation for limiting the material usage. The optimization is performed by solving the time evolutional equation that can lead to initial-independent results. The design example of a SPM motor is provided to investigate the effectiveness of the proposed method and achieve an optimum rotor design that promises reduction of the vibration without deterioration of the output torque.

Manuscript received June 29, 2013 (date on which paper was submitted for review). Corresponding author: Seungjae Min (e-mail: seungjae@hanyang.ac.kr).

Digital Object Identifier inserted by IEEE

II. Problem Formulation

A. Material Modeling and Analysis

To perform a magnetic analysis, two level set functions (ϕ_1, ϕ_2) are employed as design variables for representing the structural boundaries and material properties of PM, FM and air in the rotor. Each level set function has a sign for distinguishing the different material domains (Ω_i) and the zero points for representing the structural boundaries ($\partial\Omega_i$) as follows:

$$\begin{cases} \phi_i(\mathbf{x}) > 0 & \text{for } x \in \Omega_i^+ \\ \phi_i(\mathbf{x}) = 0 & \text{for } x \in \partial\Omega_i \\ \phi_i(\mathbf{x}) < 0 & \text{for } x \in \Omega_i^- \end{cases} \qquad i = 1,2 \tag{1}$$

Fig. 1 shows how to separate each material domain and express its boundaries. The characteristic function of χ_i has a value of 1 or 0 according to the sign of each level set function as follows:

$$\chi_i = \begin{cases} 0 & \text{for } \phi_i < 0 \\ 1 & \text{for } \phi_i \geq 0 \end{cases} \qquad i = 1,2 \tag{2}$$

The magnetic properties (p) such as the relative magnetic reluctivity (ν_r) and the remanent magnetic flux of PM ($\mathbf{B}_r$) are defined by the characteristic function as follows:

$$p(\chi_1, \chi_2) = \chi_1 \left[p_{\mathrm{PM}} \chi_2 + p_{\mathrm{FM}} (1 - \chi_2) \right] + p_{\mathrm{air}} (1 - \chi_1) \tag{3}$$

To calculate the magnetic force causes a deformation of the stator, the nonlinear magnetostatic analysis is performed by solving the following equation:

$$-\nu_0 \nu_r(\chi_1, \chi_2) \nabla^2 \mathbf{A} = \mathbf{J} + \nu_0 \nu_r(\chi_1, \chi_2) \left[\nabla \times \mathbf{B}_r(\chi_1, \chi_2) \right] \tag{4}$$

where $\mathbf{A}$ and $\mathbf{J}$ are the magnetic vector potential and the input current matrix, respectively. By using the discrete values of the characteristic function, each material region can express only a single material. Hence the magnetic analysis can be solved with clear structural boundaries and the magnetic properties of each material. The magnetic local forces calculated from the governing equation bring out the mechanical deformation of the stator, as shown in Fig. 2.

FIG. 1 HERE
FIG. 2 HERE

B. Optimization Problem Formulation

The objective function (F_j) for vibration reduction is composed of two values: the fluctuation of the magnetic force on the stator (f_j) and the driving torque (T_j) as follows:

$$F_j(\phi_1,\phi_2) = w_f F_{f,j}(\phi_1,\phi_2) + w_T F_{T,j}(\phi_1,\phi_2) = w_f \left[\frac{f_j(\phi_1,\phi_2) - f_{\text{avg},j}}{f_{\text{avg},j}} \right]^2 + w_T \left[\frac{T_j(\phi_1,\phi_2) - T_{0,j}}{T_{0,j}} \right]^2 \quad (5)$$

where f_{avg} and T_0 are the average magnetic force and the target average torque, respectively, and j a certain rotor position. It is noted that each objective function is combined with the weighting factors (w).

The optimization problem is formulated to minimize F with the volume constraints of PM (VF_{PM}) and FM (VF_{FM}) as follows:

$$\begin{cases} \underset{\phi_1,\phi_2}{\text{Minimize}}\ F(\phi_1,\phi_2) = \sum_{j=1}^{n} F_j(\phi_1,\phi_2) \\ \text{subject to } G_1(\phi_1,\phi_2) = \int_\Omega \chi_1 (1-\chi_2)\, d\Omega \Big/ \int_\Omega d\Omega \le \text{VF}_{\text{FM}} \\ \qquad\qquad G_2(\phi_2) = \int_\Omega \chi_2 d\Omega \Big/ \int_\Omega d\Omega \le \text{VF}_{\text{PM}} \end{cases} \quad (6)$$

where n is the total number of rotating position and Ω is the total design domain. By minimizing the objective function, we can reduce the fluctuation of the magnetic force by satisfying the target output torque (T_0). The average magnetic force on the stator (f_{avg}) is updated for minimizing both the fluctuation of the force and its amplitude in each design step.

C. Optimization Process

The design sensitivities of the two objective functions calculated by the adjoint variable method for reducing the computational time are combined as follows:

$$\frac{\delta F_j}{\delta \phi_i} = w_f \frac{\delta F_{f,j}/\delta\phi_i}{\max\left(\delta F_{f,j}/\delta\phi_i\right)} + w_T \frac{\delta F_{T,j}/\delta\phi_i}{\max\left(\delta F_{T,j}/\delta\phi_i\right)} \quad (7)$$

It is noted that the design sensitivity for each objective function is normalized to the same scale by dividing its maximum value. Then the level set functions are updated by solving the time evolutional equation as follows:

$$\frac{\partial \phi_i}{\partial t} = -\left(\sum_{j=1}^{n} \frac{\delta F_j}{\delta \phi_i} - \lambda_i \right) \quad (8)$$

where t is the fictitious time interval for the moving boundaries and λ is the Lagrange multiplier to satisfy the volume constraint. These processes are continued until the convergence condition is satisfied.

III. Design Example

The proposed method is applied to the rotor design of an 8-pole 12-slot SPM motor. The initial design illustrated in Fig. 3 is developed for the EPS system of which the important design target is vibration reduction. The average torque of the initial design is 3.18 Nm and its torque ripple (T_{ripple}) which is calculated by the following equation is 3.79% at the maximum rated speed of 2500 rpm.

$$T_{\text{ripple}} = \frac{T_{\max} - T_{\min}}{T_{\max} + T_{\min}} \times 100\ [\%] \quad (9)$$

The design domain is the upper side of the rotor since the lower part is bordered with the rotating shaft as shown in Fig. 3. It shows that the analysis model is set to a 1/4 partial model and has the periodic boundary conditions for the magnetic analysis. The target torque is assigned to 3.2 Nm for maintaining the output power.

FIG. 3 HERE

A. Optimal Results according to the PM Volume

The optimizations are performed with different volume fractions of PM (VF_{PM}) and the volume constraint of FM (VF_{FM}) is set to the same value (0.45) as the initial design. The weighting factors for each objective function (w_f, w_T) are fixed to 0.5 for applying the effect of each design sensitivity to the optimal shape equally.

Fig. 4 shows the optimal distribution of each material according to the PM volume, with the initial design noticed by the solid lines. It is noted that the outer surface of the PM becomes an uneven shape for adjusting the path of the magnetic flux and the airgap is increased for minimizing the magnetic force on the stator. The notches in the middle part of the PM prevent the concentration of the magnetic flux for reducing the fluctuation of the magnetic force. Instead of a clearly separated shape for each pole as the initial design, the optimal PM shapes are the long and thin shape along the tangential direction of the rotor for providing the uniform amount of the magnetic flux regardless of the rotating angle as illustrated in Fig. 5. As the volume fraction has decreased, the PM becomes divided into two parts as illustrated in Fig. 4 (b), and yet they still maintain their long, thin shape.

These optimal shapes are useful to minimize both the fluctuation and the average amount of the magnetic force (f_{avg}), as shown in Fig. 6. Table 1 summarizes that the fluctuation of the magnetic force ($\Delta f_{\text{peak to peak}}$) decreases more than 20% in all optimization cases. The torque ripple (T_{ripple}) also decreases greatly except for one case with few usage of PM ($\text{VF}_{\text{PM}} = 0.30$).

Unfortunately, such optimal shapes of PM also bring a reduction of the output power because of the wide airgap. Even if we increase the volume fraction of the PM compared to the initial design as shown in Fig. 4 (a), the optimal design barely maintain a similar level of the output torque as the initial design as summarized in Table 1.

FIG. 4 HERE
FIG. 5 HERE

FIG. 6 HERE
TABLE 1 HERE

B. Effect of the Weighting Factors

Hence, additional optimizations are performed for satisfying the target output torque. To increase the effect of $F_{T,j}$, the different value of w_T more than 0.5 is applied to the optimization. VF_{PM} and VF_{FM} are set to 0.40 and 0.45 the same as the initial design.

Fig. 7 shows the optimal rotor shape at different value for w_T. When w_T is 2.0, the boundaries of the PM become a rounded shape and the central thickness increases to provide the magnetic flux to the stator sufficiently, as illustrated in Fig. 7 (b). The FM around the edge of the PM is eliminated to reduce the leakage flux. It is confirmed that these shapes of the PM and FM help to maximize the average torque (T_{avg}) as well as to minimize the torque ripple. As w_T is decreased, the thickness of the PM is reduced and the notches appear to minimize $F_{f,j}$.

Fig. 8 shows the torque profile and fluctuation of the magnetic force on single teeth according to the weight function value. Although both the reduction of the force fluctuation and the output torque occur at the same time of necessity, we can provide several compromised designs. Table 2 demonstrates that the optimal rotor designs provide a large decrease in both the torque ripple and fluctuation of the magnetic force with only a slight loss of the output power.

FIG. 7 HERE
FIG. 8 HERE
TABLE 2 HERE

IV. CONCLUSION

This paper proposes a new design optimization method to reduce the mechanical vibration of the SPM motor. The design problem is formulated to minimize fluctuation of the magnetic force while maintaining the output torque. The design example shows a way to design a low-vibration rotor shape. It is expected that this proposed method will provide suitable design candidates at the conceptual design stage.

ACKNOWLEDGEMENT

This research was supported by Basic Science Research Program through the National Research Foundation of Korea (NRF) funded by the Ministry of Education, Science and Technology (2012R1A1B3002741) and the MKE (The Ministry of Knowledge Economy), Korea, under the CITRC (Convergence Information Technology Research Center) support program (NIPA-2013-H0401-13-1009) supervised by the NIPA (National IT Industry Promotion Agency).

REFERENCES

[1] W. Cai, P. Pillay, J. Tang and A. M. Omekanda, "Low-Vibration Design of Switched Reluctance Motors for Automotive Applications Using Modal analysis," *IEEE Trans. on Magn.*, vol. 39, no. 4, pp. 971-977, 2003.

[2] S.-H. Lee, J.-P. Hong, S.-M. Hwang, W.-T. Lee, J.-Y. Lee and Y.-K. Kim, "Optimal Design for Noise Reduction in Interior Permanent-Magnet Motor," *IEEE Trans. Ind. Appl.*, vol. 45, no. 6, pp. 1954-1960, 2009.

[3] A. Cassat, C. Espanet, R. Coleman, L. Burdet, E. Leleu, D. Torregrossa, J. M'Boua and A. Miraoui, "A Practical Solution to Mitigate Vibrations in Industrial PM Motors Having Concentric Windings," *IEEE Trans. on Magn.*, vol. 48, no. 5, 1526-1538, 2012.

[4] H.-S. Ko and K.-J. Kim, "Characterization of Noise and Vibration Sources in Interior Permanent-Magnet Brushless DC Motors," *IEEE Trans. Magn.*, vol. 40, no. 6, pp. 3482-3489, 2004.

[5] R. Islam and I. Husain, "Analytical Model for Predicting Noise and Vibration in Permanent-Magnet Synchronous Motor," *IEEE Trans. Magn.*, vol. 46, no. 6, pp. 2346-2354, 2010.

[6] J.-W. Jung, S.-H. Lee, G.-H. Lee, J.-P. Hong, D.-H. Lee and K.-N. Kim, "Reduction Design of Vibration and Noise in IPMSM Type Integrated Starter and Generator for HEV," *IEEE Trans. on Magn.*, vol.46, no.6, pp. 2454-2457, 2010.

[7] J. Hur, J.-W. Reu, B.-W. Kim and G.-H. Kang, "Vibration Reduction of IPM-Type BLDC Motor Using Negative Third Harmonic Elimination Method of Air-Gap Flux Density," *IEEE Trans. Ind. Appl.*, vol.47, no.3, pp. 1300-1309, 2011.

[8] T. Sun, J.-M. Kim, G.-H. Lee, J.-P. Hong and M.-R. Choi, "Effect of Pole and Slot Combination on Noise and Vibration in Oermanent Magnet Synchronous Motor," *IEEE Trans. on Magn.*, vol.47, no.5, pp. 1038-1041, 2011.

[9] S. Chaithongsuk, N. Takorabet and F. Meibody-Tabar, "On the Use of Pulse Width Modulation Method for the Elimination of Flux Density Harmonics in the Air-Gap of Surface PM Motor," *IEEE Trans. on Magn.*, vol.45, no.3, pp. 1736-1739, 2009.

[10] S. Lim, S. Min, T. Yamada and S. Nishiwaki, "Topology Optimization of a Magnetic Actuator Based on a Level Set and Phase-Field Approach," *IEEE Trans. on Magn.*, vol.47, no.5, pp. 1318-1312, 2011.

[11] S. Lim and S. Min, "Design Optimization of Permanent Magnet Actuator Using Multi-Phase Level-Set Model," *IEEE Trans. on Magn.*, vol.48, no.4, pp. 1641-1644, 2012.

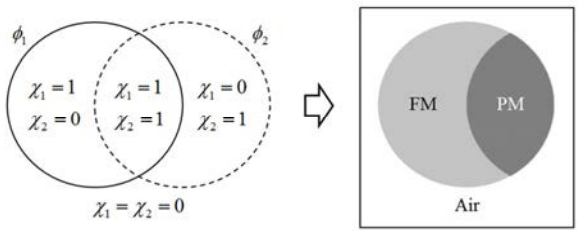

Fig. 1. Expression of multiple material domain

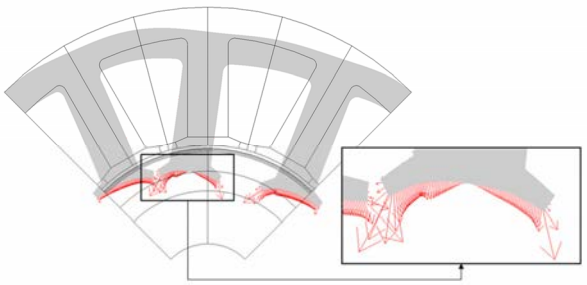

Fig. 2. Deformation of the stator due to the local magnetic force

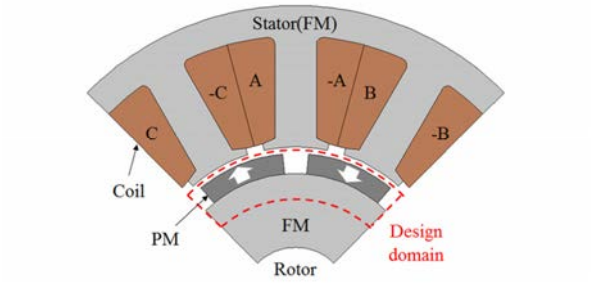

Fig. 3. Initial design of the SPM motor

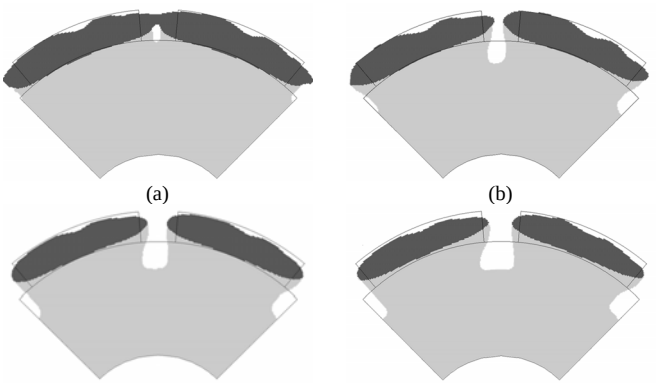

(a) (b) (c) (d)

Fig. 4. Optimal rotor design of the SPM motor according to the PM volume: (a) $VF_{PM} = 0.45$ (b) $VF_{PM} = 0.40$ (c) $VF_{PM} = 0.35$ (d) $VF_{PM} = 0.3$

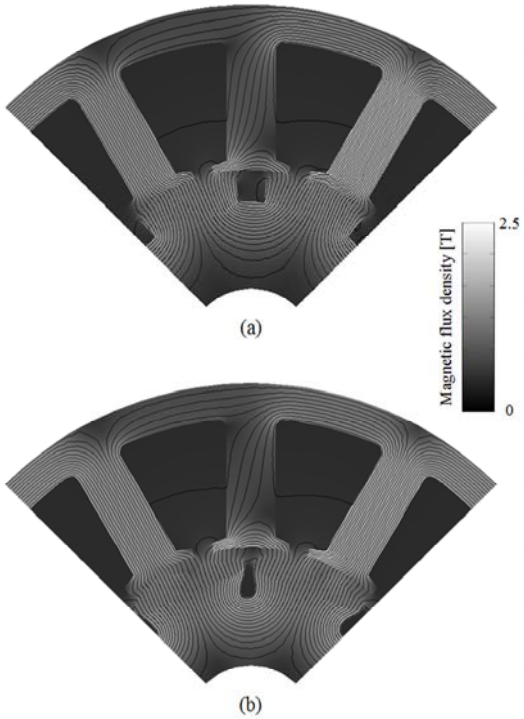

Fig. 5. Magnetic flux in the SPM motor: (a) initial design (b) optimal design ($VF_{PM} = 0.40$)

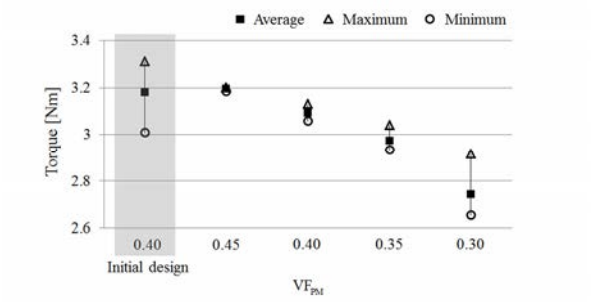

(a)

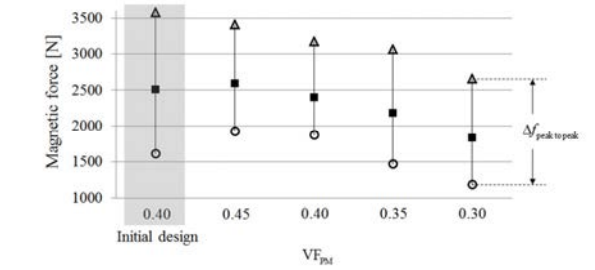

(b)

Fig. 6. Magnetic performance of the SPM motor according to the PM volume: (a) torque (b) magnetic force on single teeth

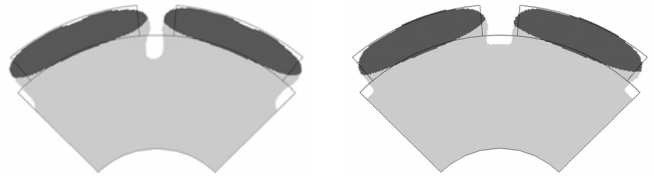

(a) (b)

Fig. 7. Effect of the weighting factor: (a) $w_T = 1.0$ (b) $w_T = 2.0$

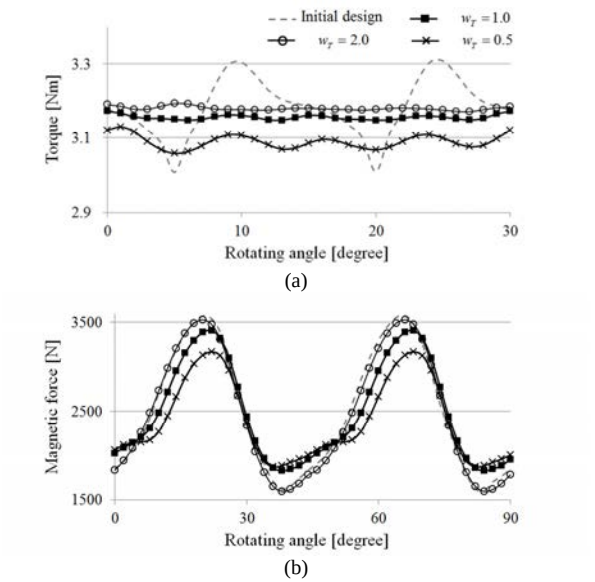

Fig. 8. Magnetic performance of the SPM motor: (a) torque profiles (b) magnetic force on single teeth

TABLE I
COMPARISON BETWEEN INITIAL AND OPTIMAL DESIGN OF SPM MOTOR

	Initial design	Optimal design			
VF_{PM}	0.40	0.45 (12.5% ↑)	0.40 (-)	0.35 (12.5% ↓)	0.30 (25.0% ↓)
T_{avg} [Nm]	3.18	3.19 (0.3% ↑)	3.09 (2.8% ↓)	2.97 (6.6% ↓)	2.74 (13.8% ↓)
T_{ripple} [%]	3.79	0.24 (93.7% ↓)	0.75 (80.2% ↓)	1.79 (52.8% ↓)	4.68 (23.5% ↑)
f_{avg} [N]	2505.1	2588.9 (3.3% ↑)	2390.9 (4.6% ↓)	2173.8 (13.2% ↓)	1829.4 (27.0% ↓)
$\Delta f_{peak\ to\ peak}$ [N]	1969.0	1481.2 (24.8% ↓)	1301.0 (33.9% ↓)	1545.5 (21.5% ↓)	1477.8 (24.9% ↓)

TABLE II
MAGNETIC PERFORMANCE ACCORDING TO THE WEIGHTING FACTOR

	Initial design	Optimal design		
		$w_T = 0.5$	$w_T = 1.0$	$w_T = 2.0$
T_{avg} [Nm]	3.18	3.09 (2.8% ↓)	3.16 (0.6% ↓)	3.18 (-)
T_{ripple} [%]	3.79	0.75 (80.2% ↓)	0.38 (90.0% ↓)	0.35 (90.8% ↓)
f_{avg} [N]	2505.1	2390.9 (4.6% ↓)	2489.5 (0.6% ↓)	2473.5 (1.2% ↓)
$\Delta f_{peak\ to\ peak}$ [N]	1969.0	1301.0 (33.9% ↓)	1562.0 (20.7% ↓)	1914.8 (2.8% ↓)